Bull. Mater. Sci., Vol. 37, No. 5, August 2014, pp. 1113–1121. © Indian Academy of Sciences.

Non-isothermal crystallization kinetics of polyethylene–clay nanocomposites prepared by high-energy ball milling

MARYAM ABARESHI[1,*], SEYED MOJTABA ZEBARJAD[2] and ELAHEH K GOHARSHADI[3,4]

[1]Chemistry Department, Payame Noor University, 19395-3697 Tehran, Iran
[2]Department of Materials Science and Engineering, Engineering Faculty, Shiraz University, Shiraz, Iran
[3]Center of Nano Research, Ferdowsi University of Mashhad, Mashhad 91775-1436, Iran
[4]Department of Chemistry, Faculty of Sciences, Ferdowsi University of Mashhad, Mashhad 91775-1436, Iran

MS received 11 June 2013; revised 4 October 2013

Abstract. **Non-isothermal crystallization kinetics of pure medium density polyethylene (MDPE) and MDPE–clay nanocomposites have been investigated by differential scanning calorimeter. The modified Avrami, Ozawa, Liu and Ziabicki equations have been applied to describe non-isothermal crystallization process. The results of Avrami analysis showed a very complicated crystallization mechanism. Although, Ozawa equation failed to provide an adequate description for non-isothermal crystallization process, Liu equation could describe it well. The data showed the crystallization rate of MDPE and nanocomposites raises with increasing cooling rate and the crystallization rate of nanocomposite is faster than that of MDPE at a given cooling rate. Ziabicki's kinetic crystallizability index showed that clay can increase the ability of MDPE to crystallize, when it is cooled at unit cooling rate. The activation energy of samples has been evaluated by Kissinger method. The results showed that the activation energy of nanocomposite was lower than that of MDPE.**

Keywords. **Differential scanning calorimeter; non-isothermal crystallization kinetics; nanocomposites; polymer.**

1. Introduction

Polyethylene (PE) is a semi-crystalline polymer. It is one of the most important thermoplastic polymers used in many industrial applications such as packaging, wire and cable industries (Hongdian *et al* 2005). The final properties of nanocomposites (NCs) based on PE, in engineering applications are critically dependent on the extent of crystallinity and nature of crystalline morphology of PE, which in turn depend on the processing conditions. Thus, it is necessary to understand the relationship between processing conditions and the development, nature and degree of crystallinity of the composites (Li *et al* 2003).

In the past decade, polymer matrix NCs have received considerable attention in both fundamental research and industry exploitation due to their unique physical and chemical properties (Xia *et al* 2006). Among these engineering group of materials, polymer–clay NCs have received much attention because of their significant properties with respect to the neat polymer such as better mechanical properties, higher thermal stability, reduced thermal expansion coefficient and gas permeability (Xu *et al* 2005).

*Author for correspondence (maryamabareshi@yahoo.com; abareshi@pnu.ac.ir)

Crystallization kinetics of semi-crystalline polymers have been continuously the subject of intense research for many decades (Apiwanthanakorn *et al* 2004; Thanomkiat *et al* 2005; Supaphol *et al* 2007). Although, the analysis for non-isothermal crystallization process may be much more complicated than that of isothermal, due to the continuous change of external conditions such as crystallizing temperature, its determination can provide plenty information on the crystalline transition (Li *et al* 2003). For example, it is very important to characterize non-isothermal crystallization behaviour of polymeric materials because these conditions are the closest to real industrial processing conditions (Liu and Wu 2002; Kim *et al* 2006).

Non-isothermal crystallization kinetics of PE and its NCs with different fillers have been extensively reported in the literature (Li *et al* 2003; Xia *et al* 2005; Xu *et al* 2005; Kim *et al* 2010). Xu *et al* (2005) investigated non-isothermal crystallization behaviours of PE–montmorillonite NCs. Their results revealed that montmorillonite has nucleation effect on crystallization of PE. Xia *et al* (2005) studied the influences of copper nanoparticles content and cooling rate on non-isothermal crystallization behaviour of low-density polyethylene (LDPE)–copper NCs. Their results indicated that both the incorporation of copper nanoparticles and cooling rates influence the crystallization behaviour of LDPE matrix

significantly. Xu *et al* (2005) prepared PE organic–montmorillonite NCs successfully via melt intercalation and studied the crystallization behaviour of PE and PE–organic montmorillonite NCs from the molten state. They concluded that the crystallization rate of PE and PE–organic-montmorillonite NCs increases with increasing the cooling rates, and the crystallization rate of PE–organic montmorillonite NCs is faster than that of PE at a given cooling rate. Kim *et al* (2010) investigated the effect of silicate dispersion on the crystallization behaviour of high density polyethylene (HDPE)–silicate composites. Their results indicated that the degree of silicate dispersion in HDPE matrix affects the nucleation activity of silicate.

In our previous work (Abareshi *et al* 2009, 2010), we successfully prepared PE–clay NCs by high-energy ball-milling method and investigated their properties. To the best of our knowledge, there is no report in the literature about non-isothermal crystallization of MDPE and MDPE–clay NCs. Thus, the main aim of the present study is to investigate non-isothermal crystallization kinetics of MDPE and MDPE–clay NCs fabricated by ball-milling method. The experimental data obtained from differential scanning calorimeter (DSC) technique were thoroughly analysed based on Avrami (1939), Ozawa (1971), Liu *et al* (1997) and Ziabicki (1967) equations, respectively. The activation energy for non-isothermal crystallization of samples was evaluated by Kissinger (1956) method.

2. Experimental

2.1 *Preparation and characterization of MDPE–clay nanocomposites*

A MDPE (density: 0·937 g cm^{-3}, MFI: 4·2, Vicat softening point: 117) was used as a matrix resin. The pristine clay used was China clay. These two commercial chemicals were used as received without further purification.

Briefly, MDPE–clay nanocomposites (PECN) were prepared by mechanical milling of MDPE and clay powders in a high-energy ball-milling. MDPE and 5, 10 and 15 wt% of clay were mechanically mixed first and then milled for different times. The same milling times were used for the neat MDPE powder. The PECN obtained containing 0·00 wt% (pure MDPE) and 15 wt% clay (PECN15) after 60 h of milling were used in this study. The details of sample preparation of PECN were reported elsewhere (Abareshi *et al* 2010).

2.2 *DSC experiments*

Non-isothermal crystallization analysis was carried out using a Perkin-Elmer Pyris-1 differential scanning calorimeter. The samples were heated up to 200 °C at the heating rate of 10 °C min^{-1}, hold it for 10 min to eliminate any previous thermal history and then cooled up to room temperature at different cooling rates of (α) of 10, 20, 30 and 40 °C min^{-1}. The exothermic curves of heat flow as a function of temperature were recorded to analyse the non-isothermal crystallization kinetics.

3. Results and discussion

3.1 *Non-isothermal crystallization behaviour*

Figure 1 shows the curve of heat flow as a function of temperature during non-isothermal crystallization for pure MDPE and PECN15 after 60 h of milling. From these curves, some useful parameters for non-isothermal crystallization analysis such as the temperature attaining 1% relative crystallinity ($T_{0.01}$), the temperature at the maximum crystallization rate, i.e. the peak temperature (T_p), the temperature for attaining 99% relative crystallinity ($T_{0.99}$), and crystallization temperature range (ΔT) can

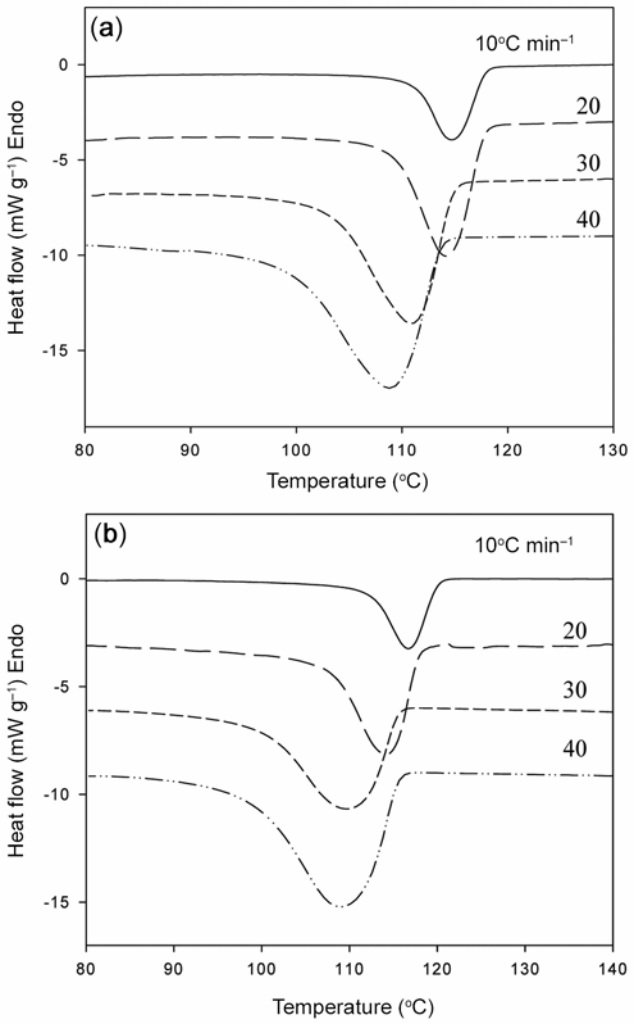

Figure 1. Non-isothermal crystallization curves for (**a**) pure PE and (**b**) PECN15 at different cooling rates.

Table 1. The values of $T_{0.01}$, T_p, $T_{0.99}$ and ΔT for pure PE and PECN15 at different cooling rates.

Sample	α (°C min^{-1})	$T_{0.01}$ (°C)	T_p (°C)	$T_{0.99}$ (°C)	$\Delta T(T_{0.99-0.01})$ (°C)
PE	10	117·73	114·11	106·88	10·85
	20	117·65	113·06	101·84	15·81
	30	114·21	108·92	95·31	18·9
	40	112·88	107·05	91·53	21·35
PECN15	10	119·92	116·21	110·39	3·71
	20	117·75	113·07	104·66	13·09
	30	114·93	108·34	97·66	17·27
	40	114·89	107·6	92·75	22·14

be obtained. The magnitude of parameters is summarized in table 1. As the cooling rate increases, the peak crystallization temperature, T_p, shifts to lower temperature and crystallization temperature range becomes broader for MDPE and PECN15. The value of T_p decreases from 114·11 to 107·05 °C for MDPE and from 116·21 to 107·6 °C for PECN15 with increasing cooling rates from 10 to 40 °C min^{-1}, which is attributed to the short time interval that allows the polymers to be crystallized with increasing cooling rate. Thus, a higher super-cooling to initiate crystallization is required and the exothermic peaks become broader. In addition, at a given cooling rate, $T_{0.01}$ and T_p of PECN15 is higher than that of pure MDPE as shown in table 1. It means that the clay acts as a nucleating agent for MDPE and accelerates the nucleation rate of polymer. Similar results have been reported in the literature for PE–organic-montmorillonite (Xu *et al* 2005) and polyamide 6-clay nanocomposites (Liu and Wu 2002).

3.2 *Non-isothermal crystallization kinetics*

The relative degree of crystallinity (X_T) as a function of temperature can be defined as follows

$$X_T = \frac{\int_{T_0}^{T} (dH_c/dT)dT}{\int_{T_0}^{T_\infty} (dH_c/dT)dT}, \quad (1)$$

where T_o and T are the temperatures at which crystallization starts and stops, respectively and dH_c/dT the heat flow rate. Figure 2 shows the relative degree of crystallinity for MDPE and PECN15 at different cooling rates. All curves have similar sigmoid shapes, indicating that only the retardation effect of cooling rate on the crystallization is observed (Ding *et al* 2007). In addition, the crystallization occurs at lower temperature with increasing cooling rate, showing at slower cooling rates, there is sufficient time to activate nuclei at higher temperatures and thus, crystallization nucleates at higher temperatures (Kim *et al* 2006).

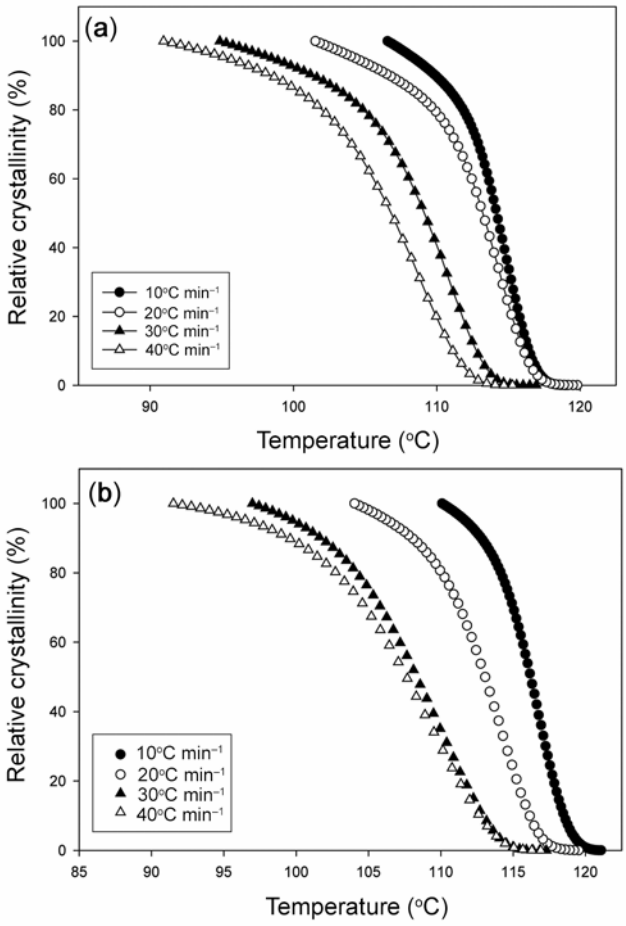

Figure 2. Relative crystallinity as a function of temperature for non-isothermal crystallization of (**a**) pure PE and (**b**) PECN15 at different cooling rates.

In non-isothermal crystallization, the temperature can be related to crystallization time, t, using the following equation

$$t = \frac{T_o - T_p}{\alpha}, \quad (2)$$

where α is the cooling rate. Thus, the temperature on the X-axis in figure 2 can be transformed into the time scale as shown in figure 3. It can be seen that the higher the

cooling rate is, the shorter time is spent for completing the crystallization process.

In order to determine the kinetics of non-isothermal crystallization process, the crystallization time at an arbitrary relative crystallinity (t_x) can be determined from the $X(t)$ functions as shown in figure 4. The values of t_x for various relative crystallinities (i.e. $x = 0{\cdot}01$, $0{\cdot}1$, $0{\cdot}3$, $0{\cdot}5$, $0{\cdot}7$, $0{\cdot}9$ and $0{\cdot}99$) for MDPE and PECN15 have been also summarized in table 2 and plotted as a function of cooling rate for MDPE and PECN15 in figure 4. The apparent total crystallization period, Δt_c, can be calculated directly from the difference between the apparent ending and the apparent onset of the crystallization process in the time domain (i.e. $\Delta t_c = t_{0{\cdot}99} - t_{0{\cdot}01}$). The values t_x and Δt_c for all the samples have been summarized in table 2. According to table 2, the value of t_x for a given value of x and the Δt_c decreases with increasing cooling rate. It suggests that non-isothermal crystallization proceeds faster with increasing cooling rate. Also, the value of t_x for a given value of X and Δt_c for PECN15 is lower than MDPE suggesting that the clay acts as a nucleating agent for MDPE and accelerates the overall crystallization process. In an attempt to further interpret the results shown in this table, plots of $\ln t_x$ vs $\ln \alpha$ are shown in figure 5. Interestingly, the linearity of these plots is evident. Table 3 summarizes value of the y-intercept and the slope obtained from these plots for all the samples. Interestingly, y-intercept of the plots was found to increase with increasing y values, $\ln t_x$, while all slopes of the plots are approximately the same. Similar results have been reported in the literature for syndiotactic polypropylene (Supaphol *et al* 2004), polytrimethylene terephthalate (Apiwanthanakorn *et al* 2004), medium-density polyethylene (Thanomkiat *et al* 2005) and isotactic polypropylene (Supaphol *et al* 2007).

3.2a *Analysis based on Avrami theory*: Several methods have been developed to describe non-isothermal crystallization kinetics of polymers. Avrami (1939) equation was modified by Jeziorny to describe non-isothermal kinetics of polymers. It has the following equation

$$1 - X = \exp(-Z_t t^n), \tag{3}$$

where the exponent n is a mechanism constant with a value depending on the type of nucleation and the growth

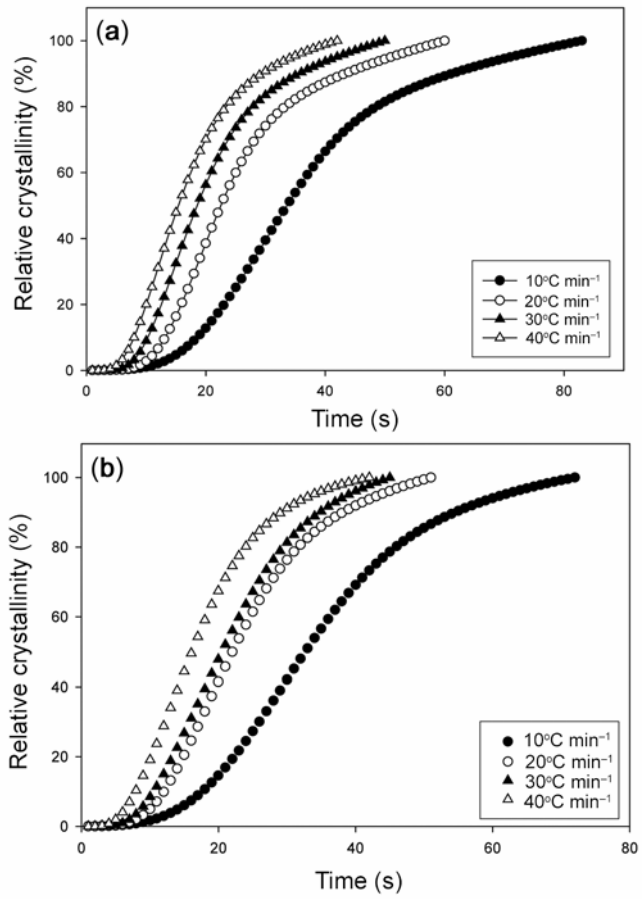

Figure 3. Relative crystallinity as a function of time for non-isothermal crystallization of (**a**) pure PE and (**b**) PECN15 at different cooling rates.

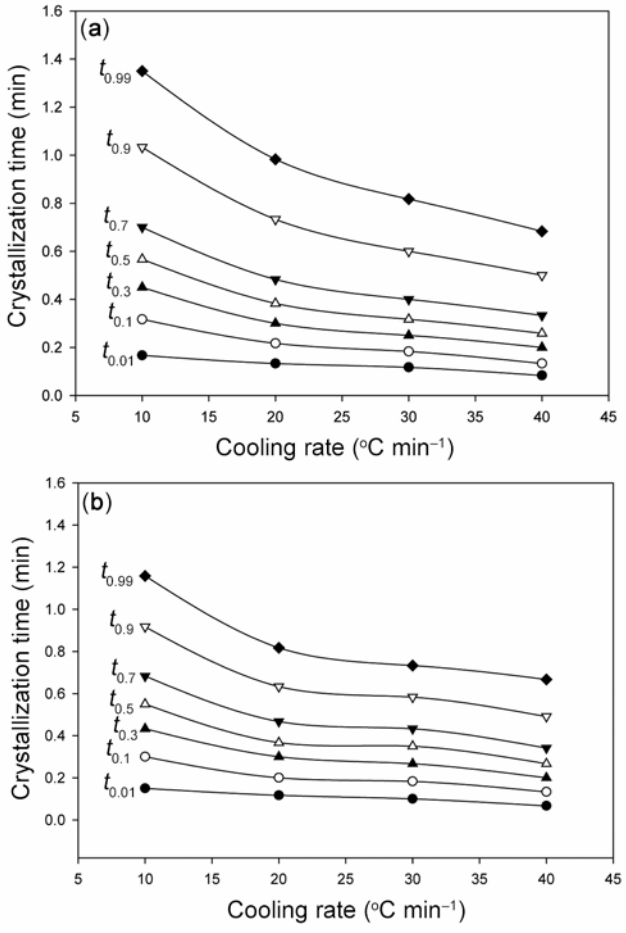

Figure 4. Crystallization time at various relative crystallinity values as a function of cooling rate for (**a**) pure PE and (**b**) PECN15.

Table 2. Quantitative analyses of the relative crystallinity function as a function of time for pure PE and PECN15 at different cooling rates.

		t_x (min)							
Sample	α (°C min^{-1})	X = 0·01	0·1	0·3	0·5	0·7	0·9	0·99	Δt_c (min)
PE	10	0·17	0·32	0·45	0·57	0·70	1·03	1·35	1·18
	20	0·13	0·22	0·30	0·38	0·48	0·73	0·98	0·85
	30	0·12	0·18	0·25	0·32	0·40	0·60	0·82	0·70
	40	0·08	0·13	0·20	0·26	0·33	0·50	0·68	0·60
PECN15	10	0·14	0·29	0·43	0·54	0·68	0·91	1·16	1·02
	20	0·11	0·20	0·29	0·37	0·46	0·64	0·82	0·70
	30	0·10	0·18	0·26	0·34	0·43	0·58	0·73	0·62
	40	0·07	0·13	0·20	0·27	0·34	0·49	0·66	0·59

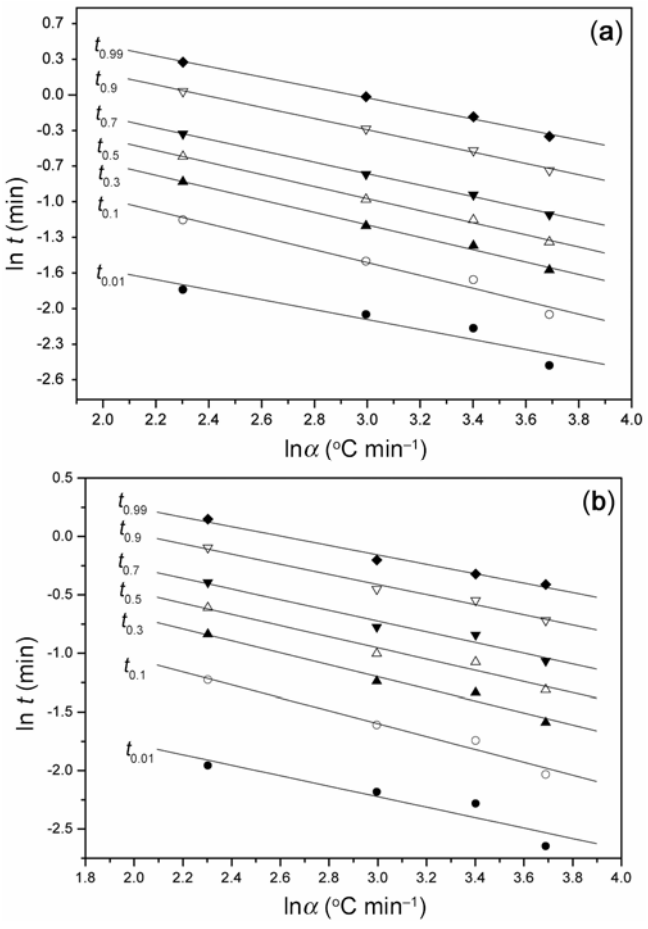

Figure 5. Crystallization time at various relative crystallinity values as a function of cooling rate for (**a**) pure PE and (**b**) PECN15.

dimension and the parameter Z_t is a growth rate constant involving both nucleation and growth rate parameters. Equation (3) can be transformed into

$$\ln[-\ln(1-X)] = \ln Z_t + n \ln t. \tag{4}$$

The Avrami exponent, n and constant, Z_t, can be obtained from the slope and intercept in the plot of $\ln[-\ln(1-X)]$ against $\ln t$ for each cooling rate, respectively. When the parameter, Z_t is corrected by the cooling rate, the reduced crystallization rate constant, Z_c, in non-isothermal crystallization is obtained

$$\ln Z_c = \frac{\ln Z_t}{\alpha}. \tag{5}$$

The plots of $\ln[-\ln(1-X)]$ vs $\ln t$ for MDPE and PECN15 are shown in figure 6. It can be seen that the plots exhibit a poor linear relationship, namely, consisting of three linear regions. It indicates that the modified Avrami analysis does not describe accurately non-isothermal crystallization of MDPE and PECN15. The kinetic parameters obtained from Avrami plots are listed in table 4. The Avrami exponent, n, in the second region is in the range of 3·48–4·59 for MDPE and 3·08–4·61 for PECN15, which means that the addition of clay influences the mechanism of nucleation and growth of MDPE crystal.

Ranganathan and Heimendahl (1981) suggested that Avrami exponent, n, can be expressed as

$$n = N_{\dim} g + B, \tag{6}$$

Table 3. Y-intercept, slope and r^2 values of regression lines drawn through plots of $\ln t_x$ against $\ln \alpha$ for various relative crystallinity values.

Sample	X	Intercept	Slope	r^2
PE	0·01	–0·69	–0·46	0·9475
	0·10	0·24	–0·59	0·9850
	0·30	0·51	–0·57	0·9972
	0·50	0·71	–0·55	0·9983
	0·70	0·86	–0·53	0·9991
	0·90	1·23	–0·52	0·9988
	0·99	1·42	–0·48	0·9981
PECN15	0·01	–0·88	–0·45	0·9345
	0·10	0·05	–0·55	0·9864
	0·30	0·34	–0·51	0·9865
	0·50	0·48	–0·48	0·9830
	0·70	0·65	–0·46	0·9828
	0·90	0·89	–0·43	0·9916
	0·99	1·05	–0·40	0·9909

Table 4. Values of Z_c and n for PE and PECN15 at different cooling rates.

		Region 1			Region 2			Region 3		
Sample	α (°C min^{-1})	n	Z_c	r^2	n	Z_c	r^2	n	Z_c	r^2
PE	10	2·19	0·36	0·9975	3·48	0·29	0·9988	1·78	0·52	0·9962
	20	2·15	0·61	0·9960	4·48	0·50	0·9982	1·60	0·77	0·9961
	30	2·50	0·70	0·9976	4·59	0·65	0·9984	1·78	0·83	0·9961
	40	2·91	0·78	0·9956	3·82	0·77	0·9953	1·74	0·88	0·9985
PECN15	10	2·19	0·37	0·9998	3·08	0·33	0·9997	2·15	0·46	0·9996
	20	2·11	0·63	0·9983	3·77	0·56	0·9993	2·02	0·72	0·9994
	30	3·12	0·68	0·9973	4·61	0·65	0·9987	2·32	0·78	0·9996
	40	3·17	0·79	0·9974	3·65	0·78	0·9969	1·97	0·86	0·9990

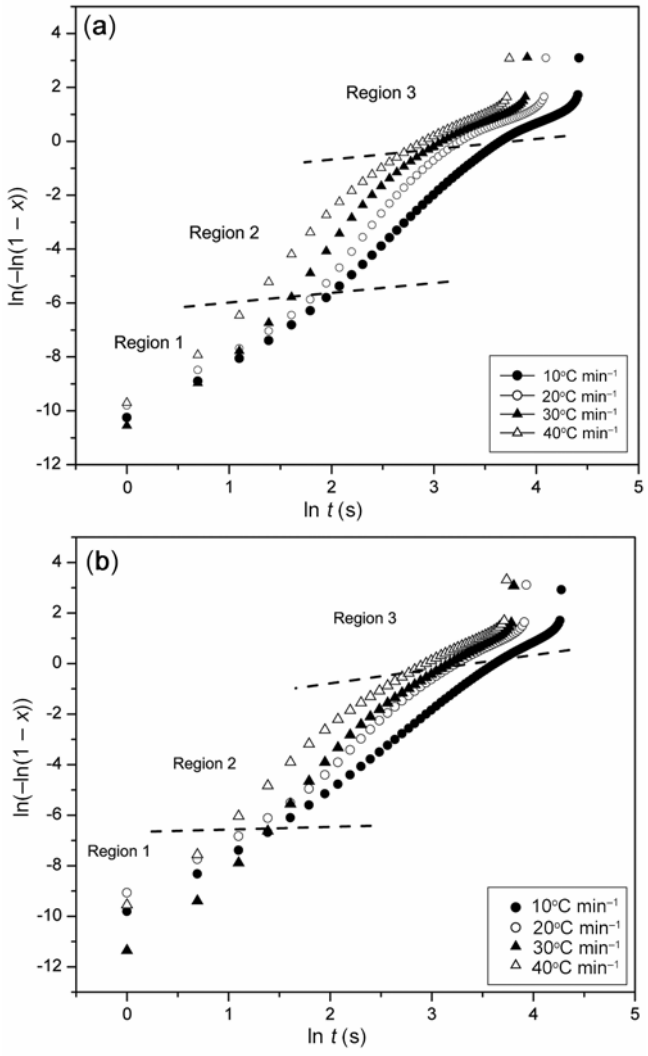

Figure 6. Avrami plots of (**a**) pure PE and (**b**) PECN15 at different cooling rates.

where B is the nucleation index ($B = 0$ for a nucleation rate of zero, $0 < B < 1$ for a decreasing nucleation rate with time, $B = 1$ for a constant nucleation rate and $B > 1$ for an increasing nucleation rate), N_{dim} the dimension of the growth (with values 1, 2 and 3 for one-, two- and three-dimensional growths, respectively) g and the growth index ($g = 1$ for interface-controlled growth and $g = 0{\cdot}5$ for diffusion-controlled growth).

For MDPE and PECN15, the value of index B was greater than 1, meaning that nucleation occurs with an increase in rate. The index, N_{dim}, was equal to 3 corresponding to a 'spherulite growth'. The value of index g was equal to 0·5 meaning a 'diffusion-controlled growth'. This suggests that the crystallization of MDPE and PECN15 occurs with an increasing nucleation rate and is governed by a three-dimensional diffusion-controlled growth. Also, it should be noted that all n values are in the ranges 3–5, implying very complicated nucleation type and growth of spherulites for these samples.

The larger the Z_c value, the larger the crystallization rate is. At the same cooling rate, the larger Z_c of nanocomposite than that of MDPE indicates that the clay prompt crystallization effectively. The effectiveness of clay as heterogeneous nuclei can also be supported by comparing Δt_c of MDPE and PECN15, which indicates that Δt_c for PECN15 is lower than that of MDPE.

3.2b *Analysis based on Ozawa theory*: Assuming that the non-isothermal crystallization process may be composed of infinitesimally small isothermal crystallization steps and occurs at a constant cooling rate. Ozawa extended the Avrami equation for non-isothermal condition as follows (Ozawa 1971)

$$1 - X = \exp\left(-\frac{K(T)}{\alpha^m}\right), \tag{7}$$

where $K(T)$ is a function of m cooling rate and m the Ozawa exponent depending on the dimension of crystal growth. The double logarithmic form of (7) gives

$$\ln[-\ln(1 - X)] = \ln K(T) - m \ln \alpha. \tag{8}$$

A plot of $\ln[-\ln(1 - X)]$ vs $\ln \alpha$ at a given temperature, results as a straight line, if the Ozawa method is valid. The kinetic parameters and $K(T)$, can be obtained from the slope and the intercept, respectively. The results based on Ozawa method for MDPE and PECN15 are shown in figure 7. It is obvious that the curves in figure 7 for MDPE

and PECN15 are not linear. Thus, the Ozawa analysis does not describe adequately the non-isothermal crystallization kinetics of MDPE and PECN15. It is well known that the Ozawa model is based on the quasi-isothermal crystallization. Non-isothermal crystallization is a dynamic process in which the crystallization rate is no longer constant, but it is a function of both time and cooling rate. In the Ozawa analysis, comparison is carried out on experimental data representing widely varying physical states of the system; however; these differences have not been taken into account in the model. For instance, for MDPE (figure 7), the data at 107 °C for cooling rate of 10 °C min^{-1} is at the very latest stage of crystallization and for cooling rate of 40 °C min^{-1} is corresponding to the point, when the crystallization just begins. Thus, if the cooling rates vary in a wide range, the Ozawa model will not be adequate in describing non-isothermal crystallization behaviour (Kissinger 1956; Li *et al* 2003; Weng *et al* 2003; Kuo *et al* 2006).

3.2c *Analysis based on Liu theory (modified Avrami–Ozawa models)*: Liu *et al* (1997) have proposed a new kinetic equation of non-isothermal crystallization by combining the Avrami and Ozawa equations. The following equation can be obtained by combining (4) and (7) under a certain crystallinity degree

$$\ln Z_t + n \ln t = \ln K(T) - m \ln \alpha, \tag{9}$$

$$\ln \alpha = \ln F(T) - b \ln t, \tag{10}$$

where $F(T) = [K(T)/Z_t]^{1/m}$ means the necessary cooling rate, when the measured system reaches certain crystallization degree at unit crystallization time. b is the ratio of Avrami exponent to Ozawa exponent, i.e. n/m. The plots of $\ln \alpha$ against $\ln t$ for MDPE and PECN15 at various crystallinity degrees are shown in figure 8. All plots show a linear relationship between $\ln \alpha$ and $\ln t$, indicating that the combined Avrami and Ozawa equations could well describe the crystallization behaviour of MDPE and PECN15. Liu equation has been also successfully used to define the crystallization kinetics for alumina-filled poly(ether ether ketone) (Kuo *et al* 2006), polyethylene–organic-montmorillonite NCs (Xu *et al* 2005), nylone 6-graphite NCs (Weng *et al* 2003), nylone 6-attapulgite NCs (Shi *et al* 2010) and polyethyleneterephthalate–clay NCs (Durmus *et al* 2010).

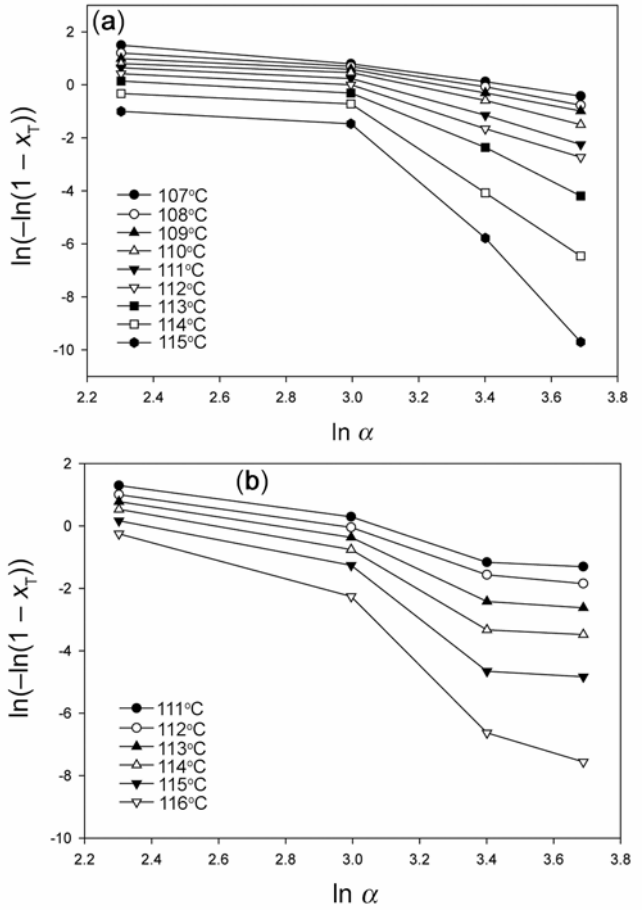

Figure 7. Ozawa plots of (**a**) pure PE and (**b**) PECN15 during non-isothermal crystallization.

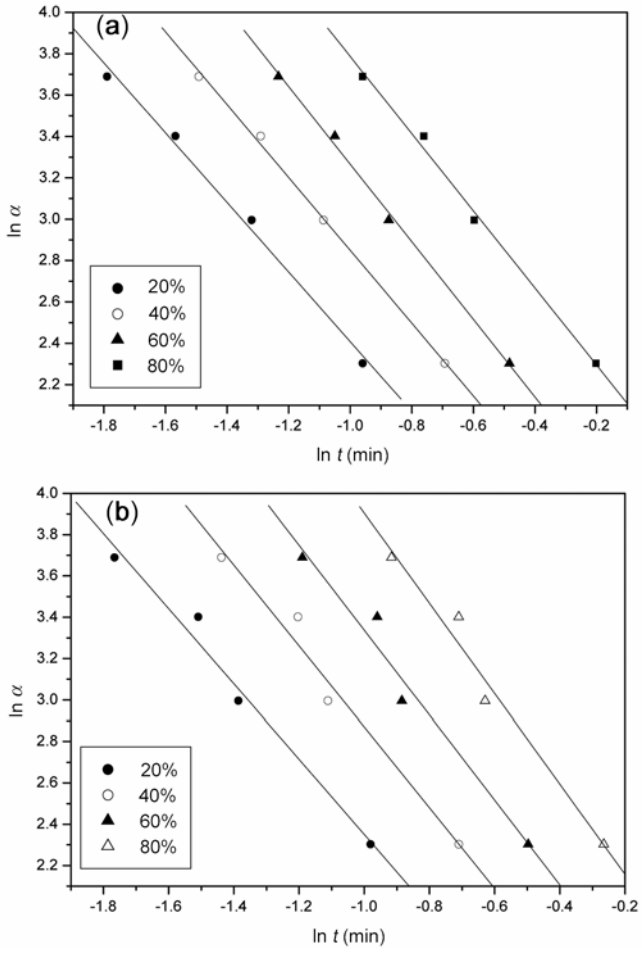

Figure 8. Plot of $\ln \alpha$ as a function of $\ln t$ for (**a**) pure PE and (**b**) PECN15 at different relative degree of crystallinity.

The values of $F(T)$ and b are listed in table 5. It is obvious that the values of $F(T)$ increases with increasing relative degree of crystallinity, indicating that at an unit crystallization time, a higher relative degree of crystallinity is obtained with a higher cooling rate. The value of b is varied from 1·68 to 1·87 and from 1·82 to 2·18 for MDPE and PECN15, respectively. These results suggest that the presence of clay as a nucleating agent influences the non-isothermal crystallization process involving the type of nucleation and crystal growth for NCs. By comparing $F(T)$ values of two samples, we found that the values of PECN15 are lower than that of pure MDPE. It means that the crystallization rate of PECN15 is faster than that of MDPE as reported for other nano-scale reinforcements (Grady *et al* 2002; Qian *et al* 2004; Kim *et al* 2006). This conclusion is consistent with the Avrami analysis.

3.2d *Analysis based on Zwieback kinetic crystallizability*: Instead of describing the crystallization process with complicated mathematical models, Ziabicki (1967) proposed that the kinetics of polymeric phase transformation can be described by a first-order kinetic equation of the form

$$\frac{\mathrm{d}X(t)}{\mathrm{d}t} = K_z(T)[1 - X(t)], \tag{11}$$

where $K_z(T)$ is a temperature-dependent crystallization rate function. In the case of non-isothermal crystallization, both $X(t)$ and $K_z(T)$ vary and depend on the cooling rate. For a given cooling condition, Ziabicki (1967) showed that the crystallization rate function, $K_z(T)$, can be described by a Gaussian function of the following form

$$K_z(T) = K_{z,\max} \exp\left[-4\ln 2 \frac{(T - T_{\max})^2}{D^2}\right], \tag{12}$$

where $T_{\max}$ is the temperature at which the crystallization rate is maximum, $K_{z,\max}$ the crystallization rate at $T_{\max}$, and D the width at half-height determined from the crystallization rate function. With the use of the iso-kinetic approximation, integration of (12) over the whole crystallizable range (i.e. $T_g < T < T_m^o$) leads to an important characteristic parameter describing the crystallization ability of a semi-crystalline polymer, i.e. kinetic crystallizability index, G_z

$$G_z = \int_{T_g}^{T_m^o} K_z(T)\mathrm{d}T \approx 1{\cdot}064 K_{z,\max} D. \tag{13}$$

The parameter G_z describes the ability of a semi-crystalline polymer to crystallize, when it is cooled at an unit cooling rate (Apiwanthanakorn *et al* 2004).

In the case of non-isothermal crystallization studies using DSC, (13) can be applied, when the crystallization rate function, $K_{Z(T)}$ replaces with the derivative function of the relative crystallinity, $(\mathrm{d}X/\mathrm{d}T)_\alpha$, which is specific for each cooling rate studied. Therefore, (13) is replaced by

$$G_{z,\alpha} = \int_{T_g}^{T_m^o} (\mathrm{d}X/\mathrm{d}T)_\alpha \mathrm{d}T \approx 1{\cdot}064 (\mathrm{d}X/\mathrm{d}T)_{\alpha,\max} D_\alpha, \tag{14}$$

where $(\mathrm{d}X/\mathrm{d}T)_{\alpha,\max}$ and D_α are the maximum crystallization rate and the width at half-height of the $(\mathrm{d}X/\mathrm{d}T)_\alpha$ function. According to (13), $G_{z,\alpha}$ is the kinetic crystallizability index for an arbitrary cooling rate. Ziabicki kinetic crystallizability index, G_z, can therefore be obtained by normalizing $G_{z,\alpha}$ with α (i.e. $G_z = G_{z,\alpha}/\alpha$). This procedure was first realized by Jeziorny.

Table 6 summarizes the values of $T_{\max}$, $(\mathrm{d}X/\mathrm{d}t)_{\max}$, D_α, $G_{z,\alpha}$ and G_z for PE and PE–clay nanocomposite. Table 6 shows that the $T_{\max}$ decreases, while the values of $(\mathrm{d}X/\mathrm{d}t)_{\max}$, D_α and $G_{z,\alpha}$ increase with increasing cooling rate. After normalizing $G_{z,\alpha}$ value with the cooling rate, the value of kinetic crystallizability at constant cooling rate, G_z, can be determined and the results are summarized in table 6. The normalized G_z values obtained for MDPE and PECN15 at different cooling rates were almost identical. The average value of G_z for MDPE and PECN15 is 0·79 and 0·87, respectively. It means that clay can increase the ability of MDPE to crystallize when it is cooled at constant cooling rate from the molten state.

Table 5. Values of $F(T)$ and b for pure PE and PECN15 at different relative degrees of crystallinity.

Sample	X (%)	$F(T)$	b	r^2
PE	20	0·72	1·68	0·9965
	40	1·09	1·76	0·9989
	60	1·39	1·87	0·9985
	80	1·92	1·86	0·9974
PECN15	20	0·53	1·82	0·9899
	40	0·91	1·95	0·9872
	60	1·28	2·05	0·9842
	80	1·72	2·18	0·9872

3.3 *Activation energy for non-isothermal crystallization*

The activation energy for non-isothermal crystallization can be derived from the combination of cooling rate and crystallization peak temperature. Kissinger (1956) suggested a method for calculating the activation energy for non-isothermal crystallization as follows

$$\frac{\mathrm{d}[\ln(\alpha/T_p^2)]}{d(1/T_p)} = -\frac{\Delta E_a}{R}, \tag{15}$$

where R is the universal gas constant and ΔE the activation energy at different cooling rates. From the slope of the plot $\ln(\alpha/T_p^2)$ vs $1/T_p$, it is found that the absolute

Table 6. Values of different kinetic parameters for pure PE and PECN15 based on Ziyabaki analysis.

Sample	α (°C min^{-1})	T_{max} (°C)	$(dX/dt)_{max}$ (s^{-1})	D_α (°C)	$G_{z,\alpha}$ (°C min^{-1})	G_z
PE	10	114·6	0·03	4·22	7·96	0·80
	20	114·3	0·05	5·40	16·05	0·80
	30	110·7	0·05	7·04	23·24	0·77
	40	108·8	0·06	8·68	31·76	0·79
PECN15	10	116·6	0·03	4·32	8·31	0·83
	20	114·3	0·04	6·24	17·03	0·85
	30	109·5	0·04	9·97	27·06	0·90
	40	108·3	0·05	10·63	35·25	0·88

values of crystallization activation energy are 241·37 and 195·10 kJ mol^{-1} for MDPE and PECN15, respectively. The activation energy of non-isothermal crystallization of PECN15 is lower than that of pure MDPE, showing that the clay acts as a nucleating agent and accelerates the non-isothermal crystallization of MDPE. Similar results have been reported for high density polyethylene–silica NCs (Kim *et al* 2010) and polypropylene–Mg–Al layered double hydroxide NCs (Ardanuy *et al* 2008).

4. Conclusions

Non-isothermal crystallization of pure MDPE and PECN15 were investigated using differential scanning calorimeter. The cooling rate was chosen 10, 20, 30 and 40 °C min^{-1}. By increasing cooling rate, the crystallization exotherms for two samples become wider and shift towards a lower temperature. The T_p for PECN15 was greater than that of the neat MDPE and Δt_c was lower than that of MDPE. It suggests that the clay acts as an effective nucleating agent for MDPE.

Non-isothermal crystallization kinetics of the samples was analysed with various kinetic models, namely, the modified Avrami, Ozawa and Liu equations. The kinetic analysis indicated that the Ozawa equation cannot provide an adequate description of the non-isothermal crystallization of MDPE and PECN15. However, the Liu method could describe well the non-isothermal crystallization of samples. The exponent, n, in the range of 3–5 indicated a very complicated crystallization mechanism, which plays role in these samples. In the Avrami method, we have found Z_c of PECN15 are larger than those of pure MDPE, which shows that the crystallization rate of PECN15 is faster than that of pure MDPE. From the Liu method, it was found that the $F(T)$ for PECN15 is lower than that of pure MDPE, indicating the crystallization rate of PECN15 is higher than that of pure MDPE, in agreement with the Avrami analysis results. Moreover, the calculation of Ziabicki kinetic crystallizability index for MDPE and PECN15 showed that clay can increase the ability of MDPE to crystallize, when it is cooled at unit cooling rate from the molten state. Finally, the crystallization activation energy of PECN15 was determined by Kissinger method.

References

Abareshi M, Zebarjad S M and Goharshadi E K 2009 *J. Compos. Mater.* **43** 2821

Abareshi M, Zebarjad S M and Goharshadi E K 2010 *J. Vinyl Addit. Technol.* **16** 90

Ardanuy M, Velasco J I, Realinho V, Arencón D and Martínez A B 2008 *Thermochim. Acta* **479** 45

Apiwanthanakorn N, Supaphol P and Nithitanakul M 2004 *Polym. Test* **23** 817

Avrami M 1939 *J. Chem. Phys.* **7** 1103

Ding Q, Dai WL and Zhang P 2007 *Polym. Eng. Sci.* **47** 2034

Durmus A, Ercan N, Soyubol G, Deligoz H and Kasgoz A 2010 *Polym. Compos.* **31** 1056

Grady B P, Pompeo F and Shambaugh R L 2002 *J. Phys. Chem.* **B106** 5852

Hongdian L, Yuan H, Junfeng X, Qinghong K, Zuyao C and Weicheng F 2005 *Mater. Lett.* **59** 648

Kim H J, Lee J J, Kim J C and Kim Y C 2010 *J. Ind. Eng. Chem.* **16** 406

Kim J Y, Park H S and Kim S H 2006 *Polymer* **47** 1379

Kissinger H E 1956 *J. Res. Natl. Stand.* **57** 217

Kuo M C, Huang J C and Chen M 2006 *Mater. Chem. Phys.* **99** 258

Li J, Zhou C and Gang W 2003 *Polym. Test* **22** 217

Liu X and Wu Q 2002 *Eur. Polym. J.* **38** 1383

Liu T X, Mo Z S, Wang S E and Zhang H F 1997 *Polym. Eng. Sci.* **37** 568

Ozawa T 1971 *Polymer* **12** 150

Qian J, He P, Nie K and He P 2004 *J. Appl. Polym. Sci.* **91** 1013

Ranganathan S and Heimendahl M V 1981 **16** 2401

Supaphol P, Thanomkiat P and Phillips R A 2004 *Polym. Test* **23** 881

Supaphol P, Thanomkiat P, Junkasem J and Dangtungee R 2007 *Polym. Test* **26** 20

Shi J, Yang X, Wang X and Lude L 2010 *Polym. Test* **29** 596

Thanomkiat P, Aht-ong D and Supaphol P 2005 *Polym. Test* **24** 873

Weng W, Chen G and Wu D 2003 *Polymer* **44** 8119

Xia X, Cai S and Xie C 2006 *Mater. Chem. Phys.* **95** 122

Xia X, Xie C and Cai S 2005 *Thermochim. Acta* **427** 129

Xu J, Wang Q and Fan Z 2005 *Eur. Polym. J.* **41** 3011

Ziabicki A 1967 *Appl. Polym. Symp.* **6** 1